

---

**Anežka JURČÍKOVÁ<sup>1</sup>, Miroslav ROSMANIT<sup>2</sup>****RECOMMENDATIONS FOR NUMERICAL MODELING AND  
ANALYTICAL ASSESSMENT OF A PLANAR STEEL CHS JOINT****Abstract**

The subject of this paper is to determine the load-bearing capacity of the truss-type CHS (circular hollow section) joint which is beyond the scope of use of the EN 1993-1-8 and thus standardized formulas for calculations of joint's strength cannot be applied. Assessment of that joint is performed by using the numerical modeling in ANSYS program and the analytical method recommended in the CIDECT (Comité International pour le Développement et l'Étude de la Construction Tubulaire) publication. The results from both methods are then compared. This paper contains recommendations for the creation of the FEM model and for calculation of load-bearing capacity of the CHS joint.

**Keywords**

CHS joint, numerical model, load-bearing capacity, ANSYS, Multi-Point Constraints.

**1 INTRODUCTION**

Nowadays, for the construction of halls and for spanning large distances, lattice girders or truss frames made of hollow sections are often used conveniently. Main advantages of such structures are their good static effect (biaxially symmetrical cross-section, shortening of the effective lengths, achievement of the required load-bearing capacity while preserving lightweight structure), and also their aesthetic appearance [1].

When designing the steel lattice structures, the practical problem may occur in the solution of welded joints. Design methods given by Eurocode are complicated, difficult to check and offer only limited scope of use (geometric conditions, restriction on material characteristics, only certain types of joints with given types of loads) [2]. That is why need arises to verify the behavior of joints which do not comply with the limitations given by the Eurocode.

The subject of this work is a solution of the lattice frame structure joint. Due to its geometry, this selected joint cannot be classified as any of the basic type of joints, which load-bearing capacities can be calculated according to recommendations in the EN 1993-1-8, and thus that joint cannot be exactly assessed on the basis of standard formulas for calculation of bearing capacity of welded CHS joints.

To describe the behavior of this joint, numerical modeling (using the FEM program ANSYS) and the recommended methods given in the publication „Design guide for circular hollow section (CHS) joints under predominantly static loading”, CIDECT publishing [3] were used. Mentioned publication offers more possibilities for assessment of CHS joints than the aforementioned Eurocode.

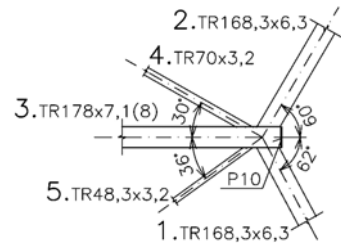
---

<sup>1</sup> Ing. Anežka Jurčíková, Department of Structural Mechanics, Faculty of Civil Engineering, VSB-Technical University of Ostrava, Ludvika Podeste 1875/17, 708 33 Ostrava, Czech Republic, phone: (+420) 597 321 391, e-mail: anezka.jurcikova@vsb.cz.

<sup>2</sup> Ing. Miroslav Rosmanit, Ph.D., Department of Building Structures, Faculty of Civil Engineering, VSB-Technical University of Ostrava, Ludvika Podeste 1875/17, 708 33 Ostrava, Czech Republic, phone: (+420) 597 321 398, e-mail: miroslav.rosmanit@vsb.cz.

## 2 DESCRIPTION OF THE STRUCTURE UNDER CONSIDERATION

In this paper it is dealt with the solution of the steel lattice frame consisting of circular hollow sections (CHS) profiles, or more accurately with the solution of the joint in a frame corner (Fig. 1.b)). The frame is axially symmetrical, and a total of six different cross-sections have been designed for this structure (I – VI in Fig. 1a)). For the cross-section No III different thicknesses of the circular hollow section were considered for the purposes of comparison, namely values  $t_0 = 7.1$  mm and  $t_0 = 8.0$  mm. These values were selected on the basis of the assessment given in the Section 3 as a result of the significantly different load-bearing capacities of the joint.



a)

b)

Fig. 1: a) Geometry of analyzed structure with types of profiles indicated;  
b) Detail of analyzed joint, including numbering of individual members.

The joint under consideration has a significant influence in the structure – it is subjected to the greatest loading and the area of the frame corner is a critical point in general terms. In addition, this joint is interesting for its geometry – considering the joint's asymmetry it cannot be classified as any of the basic type of joints for which the formulas for calculating the load-bearing capacity are given in the EN 1993-1-8. Problem with the assessment of such a joint then arises and accordingly this assessment is the aim of this work.

## 3 ASSESSMENT OF THE JOINT ACCORDING TO CIDECT RECOMMENDATION

Contrary to the Eurocode [2] the CIDECT publication [3] classifies the basic types of hollow section truss-type joints as T (which includes Y), X, or K (which includes N) based on the method of force transfer in the joint, not on the physical appearance of the joint. Definition of an X joint is then: „When the normal force component is transmitted through the chord member and is equilibrated by a brace member (or members) on the opposite side, the joint is classified as an X joint.“ [3]

According to the mentioned definition, the examined joint has been split into three simple X joints, whereas maintain the equilibrium of forces in partial joints (Fig. 2). The joints' design strengths were expressed in terms of the efficiency of the connected braces, i.e. the ratio of the axial load of the connected brace –  $N_i$  – and the joint design strength for the appropriate brace  $N_{i,Rd}$ . The resultant efficiency of the brace was then given by the summarization of efficiencies for the individual basic joints ( $X_A$ ,  $X_B$ ,  $X_C$ ). The compressed brace 1 (marking according to Fig. 1b) ) had a decisive impact on the joint's load-bearing capacity

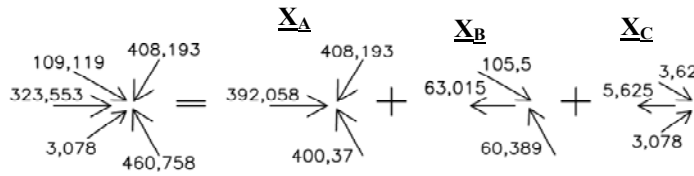


Fig. 2: Splitting of the planar joint into the combination of three simple X joints according to [3] (the values of the forces were taken from the simplified beam model of the frame).

### 3.1 General procedure to calculate design strength for chord plastification of X joint according to [3]

The design strength for chord plastification of planar X joint can be determined from the following formula, according to „Design Guide“ publication:

$$N_{i,Rd} = Q_u \cdot Q_f \cdot \frac{f_{y0} \cdot t_0^2}{\sin \theta_i} \quad (1)$$

where:

$$Q_u = 2.6 \cdot \left( \frac{1 + \beta}{1 - 0.7\beta} \right) \cdot \gamma^{0.15} \quad (2)$$

$$Q_f = (1 - |n|)^{C_1}, \text{ kde } \dots n = \frac{N_0}{N_{pl,0}} + \frac{M_0}{M_{pl,0}} \quad (3)$$

$C_1 = 0.45 - 0.25 \cdot \beta$  ... for chord compression stress ( $n < 0$ )

$C_1 = 0.2$  ... for chord tension stress ( $n \geq 0$ )

$$\beta = \frac{d_1 + d_2}{2 \cdot d_0} \quad (4)$$

$$\gamma = \frac{d_0}{2 \cdot t_0} \quad (5)$$

where:

$d_i$  – the outer diameter of the bar ( $i = 0, 1, 2$ ) [mm],

$t_0$  – thickness [mm],

$\theta_i$  – the angle between the chord and brace  $i$  ( $i = 1, 2$ ) [ $^\circ$ ],

$f_{y0}$  – chord yield stress [MPa],

$N_0; M_0$  – the internal axial force or the bending moment in connecting face [kN]; [kNm] and

$N_{pl,0}; M_{pl,0}$  – the design plastic tension or bending resistance [kN]; [kNm].

### 3.2 Resultant efficiencies and load-bearing capacities

The solved joint was split into three basic joints  $X_A$ ,  $X_B$ ,  $X_C$  (according to Fig. 2), which resultant load-bearing capacities, or efficiencies respectively are shown in tables Tab. 2 and Tab. 4. The geometry of the joint and numbering of the individual diagonals is taken from the Fig. 1b). Chord yield stress is  $f_{y,0} = 355 \text{ MPa}$ .

Tab. 1: The input values for calculating the load-bearing capacity of individual X joints for thickness  $t_{0,A} = 7.1$  mm

$\gamma = 12.535$ $A_0 = 3812 \text{ mm}^2$	$N_i$ [kN]	$N_0$ [kN]	$\beta$ [-]	$Q_u$ [-]	$n$ [-]	$C_1$ [-]	$Q_r$ [-]
$X_A$	$N_1 = 400.37$	-392.06	0.946	21.859	-0.2897	0.214	0.9295
	$N_2 = 408.193$						
$X_B$	$N_1 = 60.389$	63.015	0.669	11.934	0.0466	0.2	0.9905
	$N_4 = 105.5$						
$X_C$	$N_4 = 3.62$	5.625	0.332	6.596	0.0042	0.2	0.9992
	$N_5 = 3.078$						

Tab. 2: The resulting load-bearing capacities and efficiencies of diagonals in individual joints for thickness  $t_{0,A} = 7.1$  mm

	$N_{Rd,i}$ [kN]	$N_i/N_{Rd,i}$
$X_A$	$N_{Rd,1} = 411.807$	<b>0.9722</b>
	$N_{Rd,2} = 419.854$	<b>0.9722 &lt; 1.0 ... SATISFIED</b>
$X_B$	$N_{Rd,1} = 239.59$	<b>0.2521</b>
	$N_{Rd,4} = 423.091$	<b>0.2494</b>
$X_C$	$N_{Rd,4} = 235.882$	<b>0.0153</b>
	$N_{Rd,5} = 200,653$	<b>0.0153 &lt; 1.0 ... SATISFIED</b>

The final efficiencies of diagonals 1 and 4 for the original joint are given by the sum of efficiencies in particular X joints:

$$\frac{N_1}{N_{1,Rd}} = \frac{N_{1,XA}}{N_{1,Rd,XA}} + \frac{N_{1,XB}}{N_{1,Rd,XB}} = 0.972 + 0.252 = \underline{\underline{1.224}} > 1.0 \quad \dots \quad \text{NOT SATISFIED}$$

$(N_{Rd,1} = 376 \text{ kN})$

$$\frac{N_4}{N_{4,Rd}} = \frac{N_{4,XB}}{N_{4,Rd,XB}} + \frac{N_{4,XC}}{N_{4,Rd,XC}} = 0.249 + 0.0153 = \underline{\underline{0.265}} < 1.0 \quad \dots \quad \text{SATISFIED}$$

Tab. 3: The input values for calculating the load-bearing capacity of individual X joints for thickness  $t_{0,B} = 8.0$  mm

$\gamma = 11.125$ $A_0 = 4273 \text{ mm}^2$	$N_i$ [kN]	$N_0$ [kN]	$\beta$ [-]	$Q_u$ [-]	$n$ [-]	$C_1$ [-]	$Q_r$ [-]
$X_A$	$N_1 = 400.37$	-392.06	0.946	21.471	-0.258	0.214	0.9381
	$N_2 = 408.193$						
$X_B$	$N_1 = 60.389$	63.015	0.669	11.723	0.0416	0.2	0.9916
	$N_4 = 105.5$						
$X_C$	$N_4 = 3.62$	5.625	0.332	6.479	0.0037	0.2	0.9993
	$N_5 = 3.078$						

Tab. 4: The resulting load-bearing capacities and efficiencies of diagonals in individual joints for thickness  $t_{0,B} = 8.0$  mm

	$N_{Rd,i}$ [kN]	$N_i/N_{Rd,i}$
$X_A$	$N_{Rd,1} = 518.292$	<b>0.7725</b>
	$N_{Rd,2} = 528.42$	<b>0.7725 &lt; 1.0 ... SATISFIED</b>
$X_B$	$N_{Rd,1} = 299.098$	<b>0.2019</b>
	$N_{Rd,4} = 528.176$	<b>0.1997</b>
$X_C$	$N_{Rd,4} = 294.186$	<b>0.0123</b>
	$N_{Rd,5} = 250.25$	<b>0.0123 &lt; 1.0 ... SATISFIED</b>

The final efficiencies of diagonals 1 and 4 for the original joint:

$$\frac{N_1}{N_{1,Rd}} = \frac{N_{1,XA}}{N_{1,Rd,XA}} + \frac{N_{1,XB}}{N_{1,Rd,XB}} = 0.7725 + 0.2019 = \underline{\underline{0.974}} < 1.0 \quad \dots \quad \text{SATISFIED}$$

( $N_{Rd,1} = 473$  kN)

$$\frac{N_4}{N_{4,Rd}} = \frac{N_{4,XB}}{N_{4,Rd,XB}} + \frac{N_{4,XC}}{N_{4,Rd,XC}} = 0.1997 + 0.0123 = \underline{\underline{0.212}} < 1.0 \quad \dots \quad \text{SATISFIED}$$

#### 4 CREATION OF THE FEM MODEL

The numerical model was created in the FEM software ANSYS 12.0 using the finite elements enabling non-linear calculations (both plastic behavior of materials and influence of large deformations). For modeling the CHS profiles the shell finite element SHELL 43 was used, defined by four nodes, four thickness values and orthotropic material properties. Model of the lattice frame structure was made of the quadratic (3-node) beam element in 3-D – BEAM 189, which is defined by three nodes and a cross-section, which plane can be defined by the orientation node (node L on the Fig. 3). For the mutual connection of the BEAM and SHELL elements, the contact elements TARGE 170 (for pilot node on tip of beam interfacing with shell edge) and CONTA 175 (on the shell edge nodes) were used – see [4].

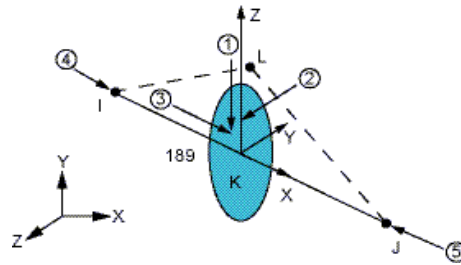


Fig. 3: Geometry of the element BEAM 189 [5].

The following material properties were assigned to the finite elements (similar to [6], [7]): Young's modulus of elasticity  $E = 210$  GPa and Poisson's ratio  $\nu = 0.3$ . The cross-sections I – VI according to Fig. 1a) were assigned to the beam elements. Both physical and geometrical non-linear aspects were considered within the calculation (plastic behavior considering the large deformations). The elasto-plastic behavior of the material was expressed by a bilinear diagram (similar to e.g., [8]) with the value of yield stress  $f_y = 355$  MPa and 5% hardening (i.e., with value of the tangent modulus  $E_2 = 10$  GPa).

To set boundary conditions, the 3D detail of the joint was interconnected with simple bar elements, by which the whole structure of a lattice frame was modeled (Fig. 4a)). The main problem of this procedure was to connect different types of finite elements – beam finite elements (BEAM 189) with shell finite elements (SHELL 43). For that interconnection aforementioned contact elements CONTA 175 and TARGE 170 were used with MPC (Multi-Point Constraints) algorithm (similar to [9]). This method enables to connect different types of finite elements quite easily and its usage has many advantages, such as:

- using MPC algorithm it is possible to solve the large deformations problem,
- there is no need to input the contact stiffness,
- either rigid constraint surface or force-distributed-surface can be used,
- the other advantage is that the CPU run time is faster and especially it is ease of use through the Contact Wizard.

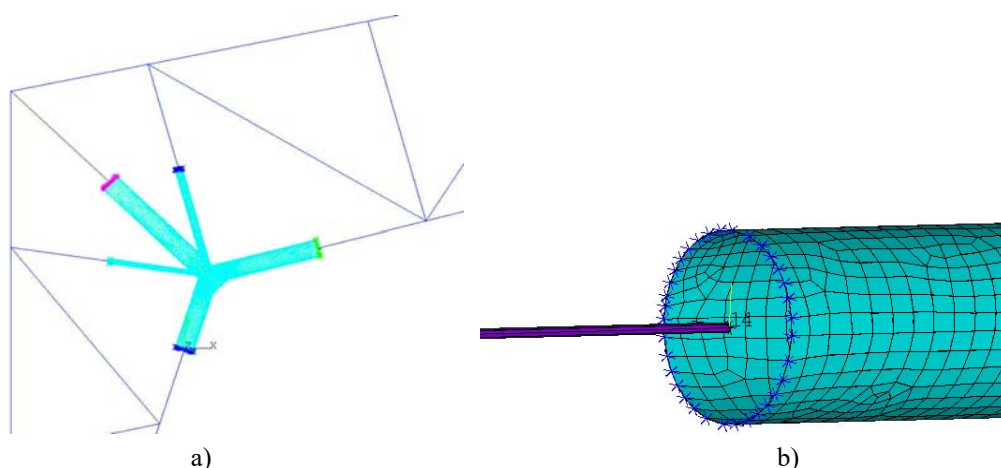


Fig. 4: a) Connection between the bar and 3D models.  
b) Detail of „Beam to Shell“ contact.

The principle of Beam to Shell MPC contact is to create node-to-surface contact pair. The node on tip of beam interfacing with the shell edge should be a pilot node (element TARGE 170). Elements CONTA 175 are then applied on nodes associated with shell edge. At the final step before creating a contact both the DOF constraints and contact surface type can be defined (it means that users can control the DOF set to be constrained with Target element and if the contact surface will be rigid or deformable). Detail of the contact is on the Fig. 4b).

Through this connection of two different types of finite elements – BEAM 189 and SHELL 43 – it was possible to specify boundary conditions (supports and loads) directly for the model of the lattice frame (Fig. 5). The behavior of the analyzed joint was thus derived from the mutual effect of the structure's individual elements, which is close to the real behavior, and so it was not necessary to seek out suitable boundary conditions for the separate detail (as in e.g., [10], [11]). The forces acting on the lattice structure were based on the critical combination of the possible load situations.

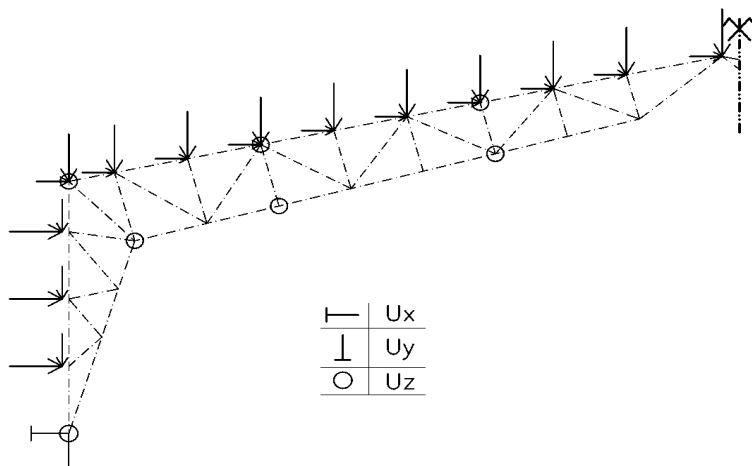


Fig. 5: Scheme of specified boundary conditions – supports and loads.

## 5 INTERPRETATION OF RESULTS

Two numerical models, which differ only in terms of the chord thickness ( $t_0 = 7.1$  mm and  $t_0 = 8.0$  mm), were studied. The models were used to observe the dependency of the chord cross-section transverse deformation on the axial force in the compressed brace 1 (the most loaded joint member) – see Fig. 6. The course of these load - deformation curves was also compared with the load-bearing capacities according to the analytical method (see Section 3) and with the deformation limit according to [12], which is  $0.01d_0$  (where  $d_0$  is chord cross-section diameter) – corresponds to serviceability strength. According to that criterion the joint strength is  $N_{Rd,1,A,def} = 348$  kN (for thickness  $t_0 = 7.1$  mm) or  $N_{Rd,1,B,def} = 414$  kN (for thickness  $t_0 = 8.0$  mm) respectively. These values correspond to the intersection of load-deformation curves from Fig. 6 with the deformation limit.

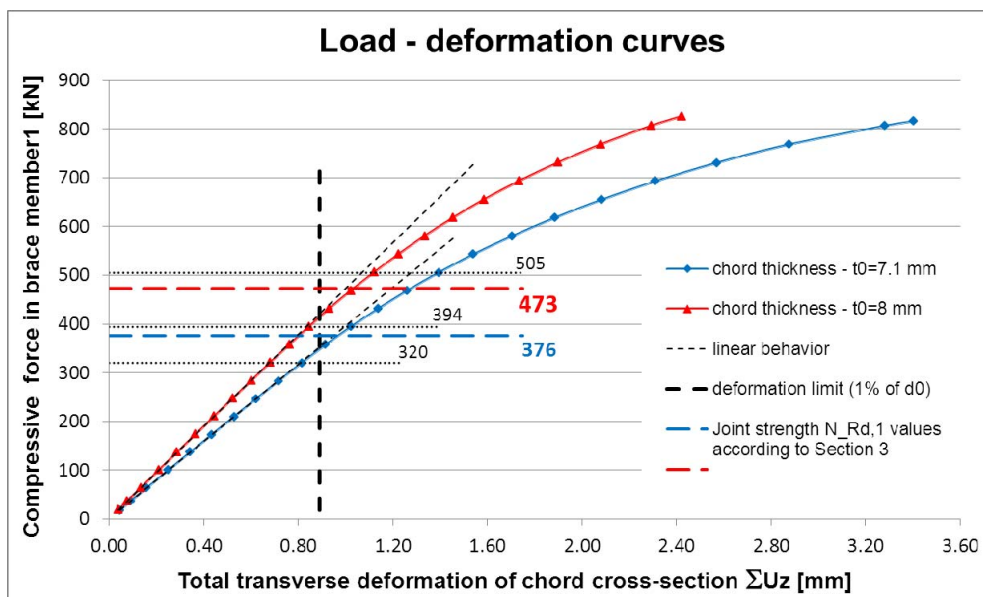


Fig. 6: Load-deformation curves for different chord thicknesses with the ultimate deformation limit  $0.01d_0$  value and with load-bearing capacities  $N_{Rd,1}$  according to Section 3.

In Fig. 7 – 9 can be observed the evolution of the stress beyond the yield stress value in three steps (see Fig. 6) – the compressive force in brace member 1 reaches the level of 320 kN, 394 kN and 505 kN. These steps represent the points before and after reaching the deformation limit  $0.01d_0$ :

- 320 kN – joint with thickness  $t_{0,A} = 7.1$  mm is before reaching deformation limit;
- 394 kN – joint with thickness  $t_{0,B} = 8.0$  mm is before reaching deformation limit;
- 505 kN – both joints are beyond this deformation limit.

In the Tab. 5 values of the chord cross-section transverse deformation ( $U_z$ ) – according to Fig. 10 – are entered on in aforementioned steps.

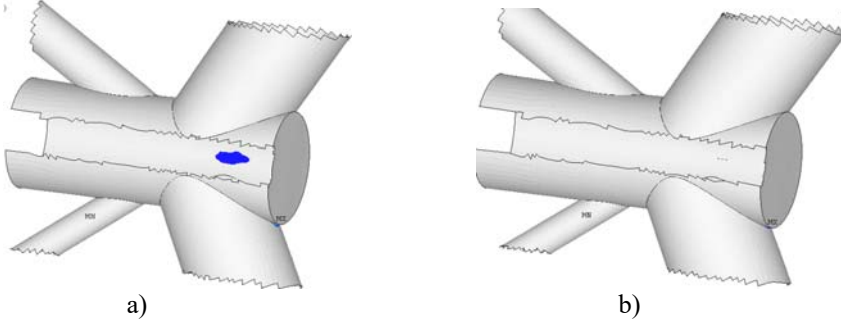


Fig. 7: Evolution of stress (von Misses) beyond the yield stress value when loaded with a force 320 kN in the brace member 1  
a) chord thickness 7.1 mm; b) chord thickness 8.0 mm

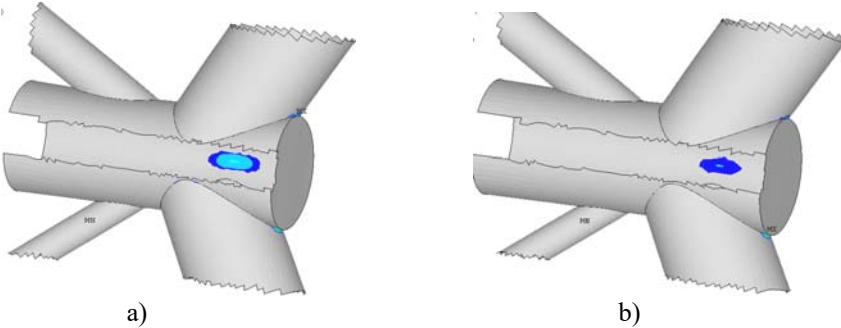


Fig. 8: Evolution of stress (von Misses) beyond the yield stress value when loaded with a force 394 kN in the brace member 1  
a) chord thickness 7.1 mm; b) chord thickness 8.0 mm

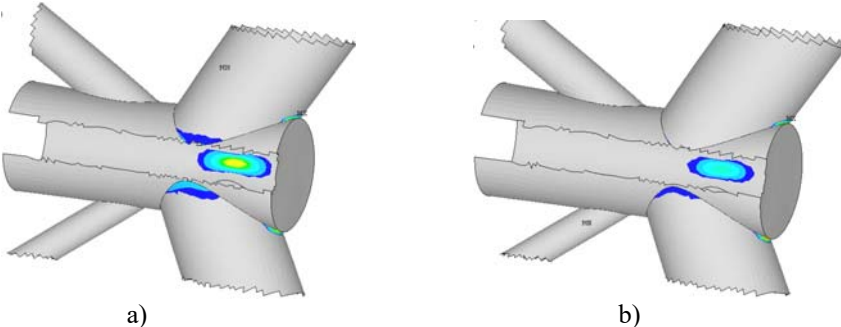


Fig. 9: Evolution of stress (von Misses) beyond the yield stress value when loaded with a force 505 kN in the brace member 1  
a) chord thickness 7.1 mm; b) chord thickness 8.0 mm



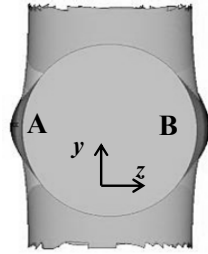


Fig. 10: Chord cross-section transverse deformation (magnified scale).

Tab. 5: Values of chord cross-section transverse deformation (see Fig. 10).

$t_0$ [mm]	$N_1$ [kN]		$U_z$ [mm]	$\Sigma U_z $ [mm]
7.1	320	A	-0.404	0.814
		B	+0.410	
	394	A	-0.508	1.022
		B	+0.514	
	505	A	-0.694	1.394
		B	+0.700	
8.0	320	A	-0.338	0.681
		B	+0.343	
	394	A	-0.421	0.846
		B	+0.425	
	505	A	-0.559	1.112
		B	+0.561	

## 6 CONCLUSIONS

A numerical model of the 3D detail of the joint, which behavior, through the contact elements (CONTA 175 and TARGE 170), is derived from the overall behavior of the structure was created. This corresponds to real behavior of the structure. The way of the joint's deformation and evolution of plastic stress corresponds to the expected failure mode, i.e., *chord plastification*. From the load-deformation curves in Fig. 6 it is evident at which load (value of the compressive force in brace member 1) the plastification of the individual joint model begins, i.e., where the curves start to deviate from the linear behavior. These values are virtually identical to the load values for the deformation limit  $0.01d_0$ , recommended in [12].

From the analytical assessment, according to [3], it is evident that a significant change in the joint load-bearing capacity (increase by 25%) can be attained by a not overly significant change in chord thickness. Used analytical method is not new (year of publication – 2008), but it is not included in design codes and is not widespread in practice. The obtained results agree well with the results from the FEM solution, which advantage is primarily giving better overview and insight on the behavior of the joint. However, the analytical method can be used better in practice, mainly due to the time-consuming preparation of numerical models with heavy demands on software knowledge.

The mismatch in the strength's values calculated using both numerical and analytical model is about 10%. This can be explained by complexity of the FE model (for example influence of the additional bending moments at the joint due to semi-rigid connection of the members). It is also questionable if the limit of the first plastification at the joint is decisive for the joint load-bearing capacity. Nevertheless it was confirmed that the recommended deformation limit is good approximation of the beginning of non-linear behavior of the joint. The problem of numerical modeling and assessment of steel welded joints will be further developed and elaborated in more detail.

## ACKNOWLEDGMENT

This research was financially supported by Project MŠMT number SP2013/169.

## REFERENCES

- [1] Wardenier, J. *Hollow Sections in Structural Applications*. CIDECT, 2001. ISBN 0-471-49912-9
- [2] *EN 1993-1-8, Eurocode 3: Design of steel structures - Part 1-8: Design of joints*. 2005.
- [3] Wardenier, J., Kurobane, Y., Packer, J. A., van der Vegte, G. J., Zhao, X. - L.: *Design guide for circular hollow section (CHS) joint under predominantly static loading*. 2nd. CIDECT, Construction with hollow steel sections, 2008. ISBN 978-393-8817-032.
- [4] *Training Manual – Advanced Contact & Fasteners for ANSYS 11.0*. First Edition, Inventory number: 002580, Published: September 22, 2008.
- [5] *Release 11.0 Documentation for ANSYS* [online]. [cit. 2013-7-15]. Available on: <<http://www.kxcad.net/ansys/ANSYS/ansyshelp>>
- [6] Salem, A. H., Soliman, E. A., Ibrahim, S. A. and Fakhry, K. F. Strength of hollow section T-joints under bending moments. In *Proceedings of Twelfth International Colloquium on Structural and Geotechnical Engineering*. Cairo – Egypt, 2007.
- [7] Jurčíková, A., Rosmanit, M.: FEM Model of Joint Consisting RHS and HEA Profiles. In: *STEEL STRUCTURES AND BRIDGES 2012: 23<sup>rd</sup> Czech and Slovak International Conference*. Podbanské, september 2012. Procedia Engineering, Volume 40, 2012, 6 p. ISSN 1877-7058.
- [8] Bittencourt, M. C., de Lima, L. R. O., Vellasco, P. C. G. da S., da Silva, J. G. S., Neves, L. F. da C.: A numerical analysis of tubular joints under static loading. In *Proceedings of APCOM'07 in conjunction with EPMESC XI*, Kyoto, Japan. December 3-6, 2007.
- [9] Jurčíková, A., Rosmanit, M.: Propojení 3D detailu styčnicku s prutovým modelem konstrukce s využitím MPC algoritmu. *Modeling in Mechanics 2013: [international conference]*, Ostrava, may 2013. Ostrava: VŠB – Technical University of Ostrava, 2013. ISBN 978-80-248-2694-3. (in Czech)
- [10] Vegte, G. J. van der, Makino, Y., Wardenier, J. The influence of boundary conditions on the chord load effect for CHS gap K-joints. In *Connections in Steel Structures*. Amsterdam. June 3-4, 2004.
- [11] Choo, Y. S., Qian, X. D., Wardenier, J. Effects of boundary conditions and chord stresses on static strength of thick-walled CHS joints. In *Journal of Constructional Steel Research*. April 2006, Volume 62, Issue 4, Pages 316–328. ISSN 0143-974X.
- [12] Lu, L. H., Winkel, G. D. de, Yu, Y., and Wardenier, J.: Deformation limit for the ultimate strength of hollow section joints. In: *Proceedings 6<sup>th</sup> International Symposium on Tubular Structures*, Melbourne, Australia, 1994.

## Reviewers:

Prof. Ing. Stanislav Kmet', PhD., Department of Steel and Timber Structures, Faculty of Civil Engineering, Technical University of Košice.

Doc. Ing. Jiří Kala, Ph.D., Institute of Structural Mechanics, Faculty of Civil Engineering, Brno University of Technology.